

Multi-UAV Behavior-based Formation with Static and Dynamic Obstacles Avoidance via Reinforcement Learning

Yuqing Xie^{1*}, Chao Yu^{1*✉}, Hongzhi Zang^{1*}, Feng Gao¹, Wenhao Tang¹,
Jingyi Huang⁺, Jiayu Chen¹, Botian Xu⁺, Yi Wu^{1,2}, Yu Wang^{1✉}

Abstract—Formation control of multiple Unmanned Aerial Vehicles (UAVs) is vital for practical applications. This paper tackles the task of behavior-based UAV formation while avoiding static and dynamic obstacles during directed flight. We present a two-stage reinforcement learning (RL) training pipeline to tackle the challenge of multi-objective optimization, large exploration spaces, and the sim-to-real gap. The first stage searches in a simplified scenario for a linear utility function that balances all task objectives simultaneously, whereas the second stage applies the utility function in complex scenarios, utilizing curriculum learning to navigate large exploration spaces. Additionally, we apply an attention-based observation encoder to enhance formation maintenance and manage varying obstacle quantity. Experiments in simulation and real world demonstrate that our method outperforms planning-based and RL-based baselines regarding collision-free rate and formation maintenance in scenarios with static, dynamic, and mixed obstacles.

I. INTRODUCTION

The formation control of multiple UAVs has received significant attention, showing great potential in practical applications such as search and rescue missions [1] and payload transport [2]. Prior studies on formation control can be sorted into three broad categories: leader-follower, virtual-structures, and behavior-based formation [3]. The leader-follower approach relies heavily on the leader; if the leader fails, the entire formation is compromised. The other two categories operate in a decentralized manner. In the virtual-structures method, UAVs follow individual reference targets to form a rigid formation, which restricts their flexibility. In contrast, behavior-based formation offers greater adaptability, since UAVs follow the formation’s centroid rather than individual reference points. Meanwhile, UAVs aim to maintain specified formation, avoid collisions with obstacles and other UAVs, and reach designated targets.

Compared with planning-based techniques [4], [5], multi-agent reinforcement learning (MARL) can produce more flexible behaviors, showing promise in solving difficult robotic tasks that require aggressive maneuvers. Some research has successfully applied MARL to formation control with static

obstacle avoidance in ground vehicles [6], [7]. Other studies use MARL for multi-UAV formation without considering obstacle avoidance [8], [9], [10]. Additionally, some work has employed RL to manage low-level actions, such as per-rotor thrusts, achieving robust obstacle avoidance without formation [11], [12]. In this paper, we tackle the more challenging task of maintaining behavior-based formation for multiple UAVs while avoiding both static and dynamic obstacles during directed flight via MARL. The primary challenges include:

- Multi-objective optimization. The policy must balance several goals: achieving directed flight, maintaining behavior-based formation, avoiding static and dynamic obstacles, and preventing collisions with each other. These goals might conflict with each other in certain scenarios, making it challenging to design a reward function that incorporates the necessary trade-offs.
- Large exploration space. The 3D nature of UAVs and task’s complexity considerably increase the exploration space.
- Sim-to-real gap. This critical issue is magnified when RL generates low-level UAV instructions for high mobility to avoid dynamic obstacles.

To address these challenges, we propose a novel two-stage RL training pipeline. In the first stage, we search for a linear utility function to balance four objectives, three for behavior completion and one for bridging the sim-to-real gap. In a simpler scenario, we evaluate the performance of different utility functions and select the one that best aligns with our preference. In the second stage, we apply the selected utility function to tackle a more complex task setting. Curriculum learning (CL), which progressively increases task difficulty, is utilized to accelerate training and enhance final performance. Additionally, we design an attention-based observation encoder to improve formation maintenance among multiple UAVs and to manage varying numbers of both dynamic and static obstacles.

Our experiments, carried out in both simulation and real-world environments, demonstrate that our method outperforms both planning-based and RL-based baselines regarding collision-free rate and formation maintenance when avoiding static, dynamic, and mixed obstacles. We also conduct ablation studies on CL and the attention-based observation encoder to validate the effectiveness of the design. Animated demonstrations can be viewed at our project website: <https://sites.google.com/view/uav-formation-with-avoidance/>.

* Equal Contributions.

✉ Corresponding Authors. {yuchao, yu-wang}@tsinghua.edu.cn

+

+ Work done as an intern in Tsinghua University.

¹ Tsinghua University, Beijing, 100084, China.

² Shanghai Qizhi Institute.

This research was supported by National Natural Science Foundation of China (No.62406159, 62325405), Tsinghua University Initiative Scientific Research Program, Tsinghua-Meituan Joint Institute for Digital Life, Beijing National Research Center for Information Science, Technology (BNRist) and Beijing Innovation Center for Future Chips, Postdoctoral Fellowship Program of CPSF under Grant Number GZC20240830, China Postdoctoral Science Special Foundation 2024T170496.

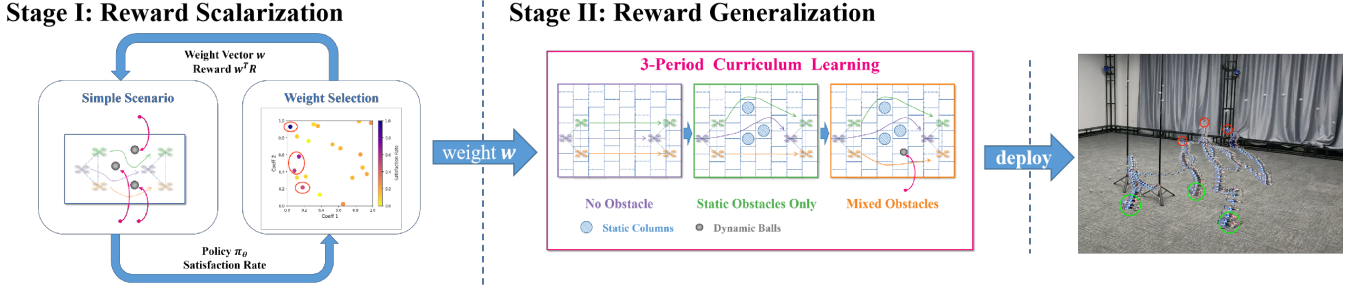


Fig. 1: Illustration of the proposed two-stage training pipeline. In the first stage, we randomly search within the reward function space to find the best weight vector that balances all four objectives. The second stage applies the reward function to a more complex scenario and solves the transformed single-objective task with curriculum learning.

II. RELATED WORK

A. Multi-UAV Formation

Extensive research has been conducted on multi-UAV formation. Classical planning-based methods [4], [5] and emerging learning-based methods [8], [9], [10], [13] guide UAVs to form a desired formation from random initial positions. Compared to the leader-follower scheme [14], [15], fully decentralized methods [16], [17], [18], [19] offer better scalability and resiliency to partial failures. However, these algorithms only consider obstacle-free or static-obstacle-only scenarios and do not account for sudden, dynamic obstacles such as flying birds. Additionally, some RL-based methods focus on navigating through static obstacles while maintaining formation for ground vehicles [6], [7]. In this paper, we derive an RL policy for behavior-based formation control in a fully decentralized manner. Transitioning from 2D to 3D space significantly increases the exploration space for RL algorithms, while extending from static to dynamic obstacles imposes higher demands on obstacle avoidance strategies.

B. Collision Avoidance for UAV

Obstacle avoidance is fundamental for UAVs in completing safe flights in cluttered environments. Methods like PANTHER [20] and Deep-PANTHER [21] effectively navigate a single UAV through obstacle-rich environments. In multi-UAV scenarios, UAVs must avoid various obstacles and potential collisions with other UAVs. Planning-based approaches utilize gradient-based optimization [22], [23], [24], evolutionary optimization [25], or particle swarm optimization [26] to plan collision-free paths for multi-UAVs in constrained environments like forests. However, these methods are designed for static environments, while real-world scenarios involve dynamic obstacles. Dynamic obstacle avoidance is particularly challenging, requiring UAVs to respond quickly to sudden obstacles and perform aggressive maneuvers [27], [28]. Planners typically need additional knowledge of obstacle trajectories, either given [29], [30] or predicted [31], [32], [33], for predictive planning. Although planning-based methods guarantee collision-free trajectories and can run in real-time, they constrain UAV behavior and may cause deadlocks. On the other hand, RL shows promise in overcoming these limitations for multi-UAV collision avoidance. [11] trains an RL policy to control motor thrust for

multi-UAV tracking in obstacle-free environments, which can be adapted to collision avoidance by modeling obstacles as UAVs. Similarly, [12] treats multi-UAV collision avoidance as a single UAV obstacle avoidance problem. In this paper, we employ RL to tackle the complex task of multi-UAV collision avoidance in mixed obstacle scenarios while maintaining formation. We use multi-objective reinforcement learning to find the best weight between multiple objectives in simple scenarios and then apply the multi-objective weight to a more challenging setting, therefore balancing computation requirement and policy efficacy.

III. TASK

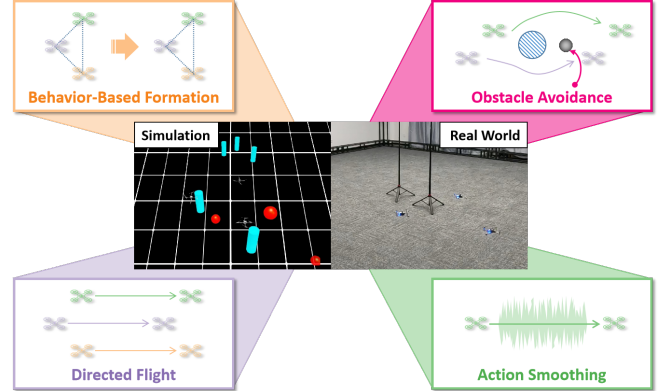


Fig. 2: Our task inherently contains four objectives: directed flight, behavior-based formation, obstacle avoidance, and action smoothing.

A. Task Setup

We address the task of maintaining behavior-based formation for multiple drones while avoiding both static and dynamic obstacles during directed flight. The task aims to achieve four objectives:

- **Directed Flight.** The drones should fly together in a specified direction. Here we use target velocity as the command.
- **Behavior-based Formation.** The drones should maintain a pre-set formation shape and size but can rotate the arrangement. For agile obstacle avoidance, the drones will not receive manually given target positions; rather,

they have to determine their own positions based on the formation centroid and other drones' status.

- **Obstacle Avoidance.** The drones must avoid all environment obstacles, both dynamic and static, and prevent collisions with each other. The static obstacles are columns with radius of **0.15m** and height of 3m. The dynamic obstacles are balls with radius of **0.15m**, moving in a parabolic trajectory towards a random drone.
- **Action Smoothing.** To facilitate zero-shot sim-to-real transfer and reduce energy consumption, the policy should generate smooth and consistent action commands.

Each objective corresponds to a reward function as detailed on the website. Together, they compose the reward vector $\mathbf{R} = (R_{formation}, R_{flight}, R_{obstacle}, R_{action})$.

B. Observation Space

The observation \mathbf{o}^i for drone i consists of the information of itself (\mathbf{o}_{self}), other drones (\mathbf{o}_{drones}), and obstacles (\mathbf{o}_{static} and $\mathbf{o}_{dynamic}$). \mathbf{o}_{self} consists of its position, orientation, linear and angular velocity, relative velocity compared to the reference velocity, and identifier. \mathbf{o}_{drones} covers the L2 distance, relative position, and relative velocity of other drones relative to drone i . \mathbf{o}_{static} uses a 3×3 distance matrix to extract the relative position of the nearest obstacle, as proposed in [34]. $\mathbf{o}_{dynamic}$ includes the L2 distance, relative position, relative velocity, and absolute velocity of the obstacle.

C. Action Space

Inspired by [35], we adopt collective thrust and body rates (CTBR) commands as policy actions to ensure robust sim-to-real transfer and agile control. These CTBR commands are subsequently converted to motor thrust commands using PID controllers. Concretely, the action for drone i is expressed as $\mathbf{a} = (c, \omega_{roll}, \omega_{pitch}, \omega_{yaw})$, where $c \in [0, 1]$ indicates the collective thrust, and $\omega \in [-\pi, \pi]$ signifies the body rates for the corresponding axes.

IV. PRELIMINARY

Our task inherently involves multi-agent cooperation and multi-objective optimization. Therefore, to model our task, we extend the definition of Markov decision processes as multi-objective, decentralized, partially observable Markov decision processes (MO-Dec-POMDPs). A MO-Dec-POMDP is defined as $\langle S, A, O, \mathbf{R}, P, n, \gamma \rangle$, where $S : \mathbb{R}^{d_s}$ is the state space, $A : \mathbb{R}^{d_a \times n}$ is the joint action space, $O : \mathbb{R}^{d_{obs} \times n}$ is the partial observation space, $\mathbf{R} : S \times A \rightarrow \mathbb{R}^{d_{obj}}$ is a vector-valued reward function that generates the reward for each objective, $P : S \times A \times S \rightarrow [0, 1]$ is the transition probability from state s_t to s_{t+1} when taking joint action a_t , n is the number of agents, and γ is the discount factor for rewards. $d_s, d_a, d_{obs}, d_{obj}$ represent the dimensions of the state, action, observation, and objective, respectively.

Solving the above MDP takes two steps. Firstly, we transform the multi-objective setting to a single-objective setting through a utility function $u : \mathbb{R}^{d_{obj}} \rightarrow \mathbb{R}$ and thus obtain a scalar reward R function, $R : S \times A \rightarrow \mathbb{R}$. Then,

as the above MDP becomes a standard Dec-POMDP, we apply multi-agent reinforcement learning algorithms to find an approximate solution.

V. METHODOLOGY

In this section, we detail our two-stage RL training pipeline that addresses the multi-objective task, as illustrated in Fig. 1. In the first stage, we identify a linear utility function that optimally aligns with our preference. Then, we transition to the second stage, where we use the utility function to tackle more complex task scenarios. We utilize curriculum learning (CL) to navigate large exploration spaces and accelerate training.

We also describe the network architecture, which features an attention-based observation encoder to improve formation control and deal with different quantities of obstacles.

A. Two-Stage Training Pipeline

1) *The First Stage, Reward Scalarization:* Manually designing a reward function is difficult because the task involves multiple objectives with complex interrelationships. Therefore, we attempt to automatically transform the multi-objective reward into a scalar value. Specifically, we assume a linear utility function u , where the scalar reward R is a weighted sum of the reward components, $R = u(\mathbf{R}) = \mathbf{w}^T \mathbf{R}$, with weight vector $\mathbf{w} = (w_{formation}, w_{flight}, w_{obstacle}, w_{action})$ and reward vector $\mathbf{R} = (R_{formation}, R_{flight}, R_{obstacle}, R_{action})$. Using the weight vector \mathbf{w} , we can establish the relationship between each objective, and thereby convert the multi-objective problem into a single-objective one.

Existing multi-objective RL methods are not suitable for finding a proper \mathbf{w} , as they cannot fully explore the weight space when the value of each objective becomes highly non-monotonic with the weight. Thus, we repeatedly select a random weight vector \mathbf{w} , use the MAPPO algorithm [36] to solve the transformed Dec-POMDP, and evaluate the corresponding policy using satisfaction rate (SR) as the metric. An episode is satisfying if its four objectives meet certain thresholds, and SR is the proportion of satisfying episodes out of all testing episodes. We choose the \mathbf{w} whose corresponding policy best aligns with our preference for the second stage. In practice, we select the \mathbf{w} with the highest SR.

Unfortunately, finding an appropriate weight vector requires multiple rounds of training, which is computationally expensive and time-consuming. To expedite the convergence of MAPPO for each \mathbf{w} , we consider a simplified task: three drones maintaining a triangular formation while dodging three dynamic obstacles.

2) *The Second Stage, Reward Generalization:* In the first stage, we find a proper \mathbf{w} in a simplified setting. Now, we use the weight to scalarize the reward vector and tackle a more complex task: three drones navigating through both static and dynamic obstacles. This stage confirms the generalizability of the derived reward function and highlights the effectiveness of our proposed approach.

Training the RL policy from scratch for complex tasks is computationally intensive and often leads to suboptimal

solutions. Hence, we utilize curriculum learning to speed up the training process through gradually increasing task difficulty. Specifically, we implement a 3-period curriculum, where drones first learn to fly forward in an obstacle-free environment, followed by a static-obstacle-only environment, and ultimately a mixed-obstacle environment.

B. Network Architecture

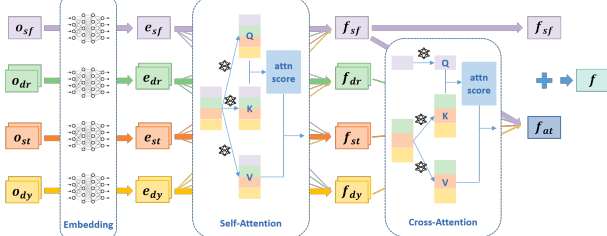


Fig. 3: The network structure of the observation encoder.

1) *Attention-Based Observation Encoder*: To efficiently manage scenarios with different quantities of obstacles, we develop an attention-based observation encoder. This encoder eliminates the limitations on input dimensionality and emphasizes relevant task information. The structure of the encoder is shown in Fig. 3. The observation composes of four parts: \mathbf{o}_{self} , \mathbf{o}_{drone} , \mathbf{o}_{static} , and $\mathbf{o}_{dynamic}$. Each part is individually encoded through separate MLPs to produce embeddings of identical dimensions. We use multi-head self-attention on these embeddings to obtain respective features. To better capture the relationships between the drone and other environmental entities, the features are processed through a multi-head cross-attention module, utilizing self-feature as the query and other features as the key and value. The final feature \mathbf{f} is a concatenation of the self-feature and the output of the multi-head cross-attention.

2) *Actor&Critic Network*: Following the observation encoder, a Gaussian distribution model $\pi_\theta = \mathcal{N}(\mu_\theta, \sigma_\theta)$ is used to parameterize actions in the actor network. Additionally, an MLP outputs a scalar value $V = V_\phi(\mathbf{f})$ as the estimated reward-to-go for the current state in the critic network.

VI. EXPERIMENTS

A. Baselines

We compare our approach with three state-of-the-art baselines that meet some objectives: Swarm-Formation [37], R-Mader [30], and Swarm-RL [34]. We outline the characteristics of the baselines in Tab. I and leave the modifications that tailor them to our task to the website. Since R-Mader and Swarm-RL do not inherently manage formation, we set the desired formation as the target positions of the drones to encourage formation maintenance.

B. Simulation Results

We choose OmniDrones [38] as our testbed, a drone simulator designed for RL policy training, thanks to its high-speed GPU simulation and complex environment dynamics for drones.

We consider a challenging task: 3 drones fly as a near-equilateral triangle while avoiding static and dynamic obstacles scattered within the space. We obtain the policy through our proposed 2-stage RL training pipeline. During the first training stage, each trial requires 100 million environment steps. During the second training stage, we perform 3-period curriculum learning, where we train the RL policy in scenarios with no obstacle, 10 static obstacles only, and mixed obstacles with 10 static and 2 dynamic obstacles, sequentially. Each period takes 15 million, 150 million, and 150 million environment steps, respectively. Swarm-RL takes 1 billion environment steps to converge, about 3x steps of our method.

1) *Evaluation Metrics*: We consider two metrics to examine the performance:

- **Collision-Free Rate (CFR)**. An episode is considered successful if drones avoid collisions with all obstacles and with each other while reaching a specified area in time. The collision-free rate is defined as the proportion of successful episodes out of the total episodes. This metric evaluates the performance of directed flight and obstacle avoidance. The higher, the better.
- **Formation Maintenance (FM)**. In successful episodes, we compute the unnormalized Laplacian distance between the target formation and the actual swarm configuration. A smaller unnormalized Laplacian distance indicates a more desirable formation in terms of both shape and size.

Note that we do not quantify the performance of action smoothing, since this term facilitates sim2real transfer, which will be verified in real-world experiments. In the following section, we report the CFR and FM of planning-based methods averaged over 25 repeated experiments, as they do not support parallel evaluation, and RL-based methods over 100 trials. The positions of all obstacles are randomly generated in each trial.

	Swarm-Formation	R-Mader	Swarm-RL	Ours
CFR(\uparrow)	0.08	0.20	0.83	0.89
FM(\downarrow)	1.353	4.052	0.959	0.278

TABLE II: Performance of all methods under mixed obstacle scenario (2 balls + 10 columns) in simulation.

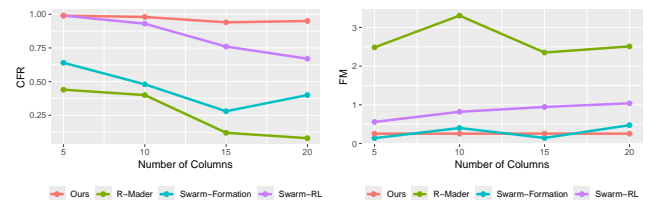


Fig. 4: Varying the number of static obstacles.

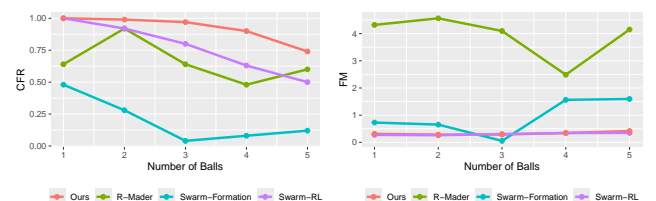


Fig. 5: Varying the number of dynamic obstacles.

Method	Type	Directed Flight	Formation Maintenance	Obstacle Avoidance	Action Type
Swarm-Formation [37]	Planning	✓	✓	Static	Trajectory
R-Mader [30]	Planning	✓	✗	Static & Dynamic (Trajectory Needed)	Trajectory
Swarm-RL [34]	RL	✓	✗	Static	Thrust
Ours	RL	✓	✓	Static & Dynamic	CTBR

TABLE I: Characteristics of baselines and our method.

2) *Main Results*: We test all methods in the mixed obstacle scenario with 2 balls and 10 columns and report the performance in Tab. II. We further test the zero-shot transfer ability of our policy by varying the number of obstacles. We gradually increase the number of columns from 5 to 20 under static obstacle scenario, and the number of balls from 1 to 5 under dynamic obstacle scenario. The results are shown in Fig. 4 and Fig. 5, respectively.

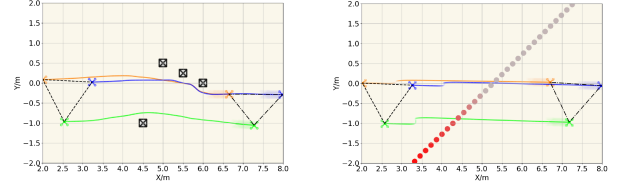
Our method outperforms all baseline methods regarding both CFR and FM in the mixed obstacle scenario, and demonstrates comparable, if not superior, performance to the best baseline in extremely confined environments with 20 columns or 5 balls. The results demonstrate our method’s strong capability to maintain effective formation while evading various obstacles, underscoring its ability to accomplish multi-objective tasks. Also, as the number of obstacles increases, our method shows only a slight decrease in both metrics, demonstrating its strong scalability and generalization capability, which we attribute to the attention mechanism employed in the network structure.

Swarm-Formation has a low CFR because it is designed for large-scale environments but not for fine-grained, dense obstacle distributions, as in our setting. It also lacks proper trajectory prediction for dynamic obstacles. Therefore, when a dynamic obstacle suddenly appears in front of a drone, the algorithm prematurely assumes a collision and ceases to control the drone.

R-Mader, which inherently incorporates dynamic obstacle avoidance, performs better in dynamic scenarios compared to Swarm-Formation, but still falls short of our method’s performance. This is because drones can only observe obstacles within a certain distance in our task setting. For R-Mader, this is equivalent to reducing the response time for obstacle avoidance.

While Swarm-RL maintains high CFR in static obstacle scenarios, its formation is easy to break: when one drone changes its behavior to avoid obstacles, other drones simply ignore it and keeps flying forward. In dynamic settings, as the number of obstacles increases, the CFR drops significantly, indicating inadequate scalability.

3) *Behavior Visualization*: In Fig. 6, we visualize the formation behavior of our method under static scenario with 4 columns (represented by black boxes) and dynamic scenario with 1 ball (represented by red circles). In static scenario, our method adjusts the centroid of the formation and slightly twists its formation, demonstrating the flexibility of behavior-based formation structure. In dynamic scenario, our method requires all drones to decelerate upon encountering the ball and resume flight after the ball drops.



(a) Static obstacle scenario. (b) Dynamic obstacle scenario.

Fig. 6: Behavior visualization. (Top view)

C. Analysis of Reward Scalarization

Fig. 7 (a) illustrates the satisfaction rates (SR) of policies trained with randomly sampled weight vectors \mathbf{w} . We observe that weight vectors with similar SR can yield diverse behaviors. Fig. 7 (b) depicts the trajectories of 3 drones dodging a dynamic obstacle, guided by policies with similar satisfaction rates. When encountering a dynamic obstacle, the first policy and the third policy decelerate the drones in different magnitudes, whereas the second policy chooses to ascend and accelerate the drones. This suggests that our method holds strong flexibility and policy diversity, allowing humans to choose behaviors that best align with their preferences. In practice, we select the weight vector with the highest SR.

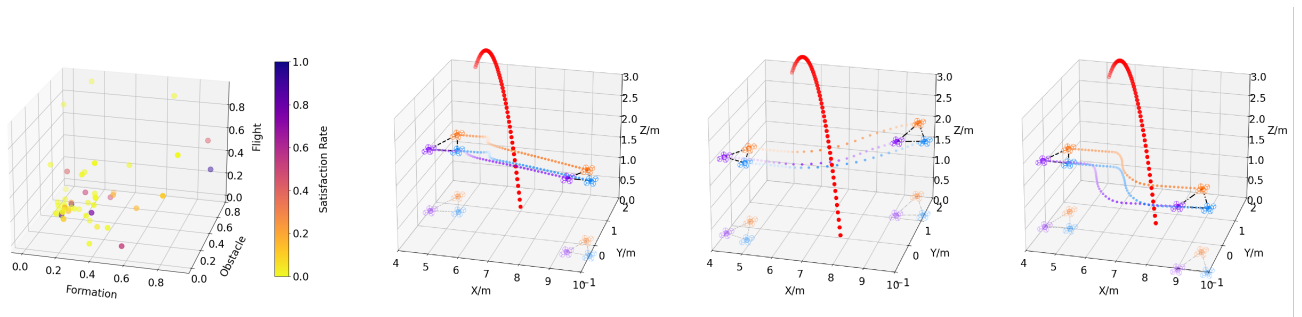
D. Ablation Studies

In this section, we conduct ablation studies on the attention-based observation encoder and CL used in the second stage. All experiments are conducted in mixed obstacle scenario with 10 columns and 2 balls. We set success criteria for each objective and record the proportion of episodes meeting these criteria. Furthermore, we use Success Rate to record the proportion of episodes meeting all criteria simultaneously.

1) *Attention-based Observation Encoder*: We compare three variants: (1) Ours w/o CA, where the cross-attention module is replaced with an MLP, (2) Ours w/o SA, where the self-attention module is replaced with an MLP, and (3) MLP, where both the cross-attention and self-attention modules are substituted with an MLP.

As demonstrated in Fig. 8, only our method exhibits satisfying success rates regarding all objectives. The variants either fail to reach the destination or collide with obstacles. This suggests that the attention modules significantly enhance the policy’s ability to handle obstacles and integrate information from other drones.

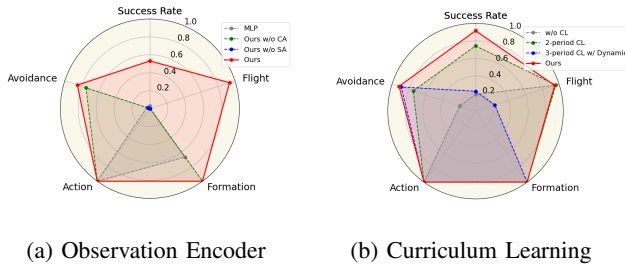
2) *Curriculum Learning*: We consider the following four curriculum designs: (1) w/o CL, which trains the policy from scratch, (2) 2-period CL, which trains the policy in obstacle-free environment, then in mixed scenarios, (3) 3-period CL w/ Dynamic, which, unlike 2-period CL, trains the policy in



(a) Satisfaction Rates

(b) Diverse Behaviors

Fig. 7: (a) The satisfaction rates under different weight vectors. The x-, y-, and z-axis represent the weight of the formation, obstacle, and flight objectives, respectively, and the weight of the action objective can be calculated as $w = 1 - x - y - z$. The darker the color, the higher the satisfaction rate. (b) Policy behaviors induced by different weight vectors. The red line represents the trajectory of the dynamic obstacle.



(a) Observation Encoder

(b) Curriculum Learning

Fig. 8: Results of the ablation studies.

dynamic scenarios before moving to mixed scenarios, and (4) Ours, which trains the policy through obstacle-free, static-obstacle-only, and mixed scenarios, sequentially.

Trained with the same amount of data, our curriculum achieves superior overall performance. Comparing the performance of 2-period CL with 3-period CL w/ Dynamic, we observe that training to avoid static obstacles enhances the ability to avoid dynamic obstacles. This is because, when trained exclusively in dynamic obstacle scenarios, drones tend to fly backwards for obstacle avoidance and therefore fail to meet the flight objective within the given time. However, with the presence of columns during training, the policy learns to alter its formation and decelerates less as balls appear.

E. Real World Deployment

We deploy our RL policy and the planning-based baselines on Crazyflie 2.0. Due to the limited processing power of Crazyflie’s onboard processors, we execute the RL policy and planning baselines on a computer, and send commands to the drones via Crazyradio. We acquire the ground truth positions of the drones and obstacles through a motion capture system and estimate their linear and angular velocities by calculating the differences in position and rotation between consecutive frames. For the RL policy, CTBR commands are transmitted via radio at 50 Hz, while for planning baselines, trajectory waypoints are sent through position commands at 10 Hz. We tried to deploy Swarm-RL both on-board and on external PC, but failed in both cases; therefore, we do not present the real-world results of Swarm-RL.

1) *Sim2Real Transfer*: For better Sim2Real transfer, we add domain randomization and CTBR clip during training.

More specifically, we randomize the initial position of each drones within 0.05m of the original formation, and randomize the initial rotation within $[-0.1\pi, 0.1\pi]$. Also, to avoid extreme actions, we clip the policy output, setting ω within $[-45, 45]$ degree/s and c within $[0.4, 0.9]$.

2) *Results and Analysis*: In real world deployment, we consider three scenarios, i.e., with 2 static columns, with a manually thrown ball, and with both the columns and the ball. For full video, please refer to the supplementary materials.

The results further demonstrate the strong Sim2Real transfer capability of our method. Our method can perform aggressive dodging strategy to safely navigate through all obstacles while maintaining formation, whereas the baseline methods fail to find a viable path. Swarm-Formation halts when the dynamic obstacle drops before the drone; R-Mader struggles with cluttered static obstacles and fails to keep formation. Through the zero-shot Sim2Real deployment, we validate the efficacy of the action smoothing objective.

VII. CONCLUSION AND FUTURE WORK

In this paper, we employ multi-agent reinforcement learning to tackle the challenging task of maintaining behavior-based formation among multiple UAVs while avoiding both static and dynamic obstacles during directed flight. Our approach involves a two-stage training pipeline. In the first stage, we search for a balanced weight of all objectives in a simplified task setting. In the second stage, we apply curriculum learning to navigate the large exploration space, deriving a feasible policy for the more complex task. We introduce an attention-based observation encoder to effectively capture the features of the drones and the environments, ensuring the scalability of the policy. Our approach outperforms SOTA baselines in terms of both CFR and FM. The effectiveness of our method is further validated through real-world deployment.

Currently, our approach assumes perfect communication between drones and is limited to a structured environment without vision-based sensing. Future improvements could involve developing a vision-based policy to handle obstacles and making the system robust to communication delays.

REFERENCES

[1] Y. Liu and G. Nejat, "Multirobot cooperative learning for semi-autonomous control in urban search and rescue applications," *Journal of Field Robotics*, vol. 33, no. 4, pp. 512–536, 2016.

[2] N. Rao, S. Sundaram, and P. Jagtap, "Temporal waypoint navigation of multi-uav payload system using barrier functions," in *2023 European Control Conference (ECC)*. IEEE, 2023, pp. 1–6.

[3] G.-P. Liu and S. Zhang, "A survey on formation control of small satellites," *Proceedings of the IEEE*, vol. 106, no. 3, pp. 440–457, 2018.

[4] Z. Lin, W. Ding, G. Yan, C. Yu, and A. Giua, "Leader–follower formation via complex laplacian," *Automatica*, vol. 49, no. 6, pp. 1900–1906, 2013.

[5] M. C. De Gennaro and A. Jadbabaie, "Formation control for a cooperative multi-agent system using decentralized navigation functions," in *2006 American Control Conference*. IEEE, 2006, pp. 6–pp.

[6] M. Dawood, S. Pan, N. Dengler, S. Zhou, A. P. Schoellig, and M. Bennewitz, "Safe multi-agent reinforcement learning for formation control without individual reference targets," *arXiv preprint arXiv:2312.12861*, 2023.

[7] Y. Yan, X. Li, X. Qiu, J. Qiu, J. Wang, Y. Wang, and Y. Shen, "Relative distributed formation and obstacle avoidance with multi-agent reinforcement learning," in *2022 International Conference on Robotics and Automation (ICRA)*. IEEE, 2022, pp. 1661–1667.

[8] Z. Liu, J. Li, J. Shen, X. Wang, and P. Chen, "Leader–follower uavs formation control based on a deep q-network collaborative framework," *Scientific Reports*, vol. 14, no. 1, p. 4674, 2024.

[9] A. Khan, E. Tolstaya, A. Ribeiro, and V. Kumar, "Graph policy gradients for large scale robot control," in *Conference on robot learning*. PMLR, 2020, pp. 823–834.

[10] T. A. Karagüzel, V. Retamal, and E. Ferrante, "Onboard controller design for nano uav swarm in operator-guided collective behaviors," in *2023 IEEE International Conference on Robotics and Automation (ICRA)*. IEEE, 2023, pp. 3268–3274.

[11] S. Batra, Z. Huang, A. Petrenko, T. Kumar, A. Molchanov, and G. S. Sukhatme, "Decentralized control of quadrotor swarms with end-to-end deep reinforcement learning," in *Conference on Robot Learning*. PMLR, 2022, pp. 576–586.

[12] X. Han, J. Wang, Q. Zhang, X. Qin, and M. Sun, "Multi-uav automatic dynamic obstacle avoidance with experience-shared a2c," in *2019 International Conference on Wireless and Mobile Computing, Networking and Communications (WiMob)*. IEEE, 2019, pp. 330–335.

[13] J. Wang, J. Cao, M. Stojmenovic, M. Zhao, J. Chen, and S. Jiang, "Pattern-rl: Multi-robot cooperative pattern formation via deep reinforcement learning," in *2019 18th IEEE International Conference On Machine Learning And Applications (ICMLA)*. IEEE, 2019, pp. 210–215.

[14] S. Zhao, "Affine formation maneuver control of multiagent systems," *IEEE Transactions on Automatic Control*, vol. 63, no. 12, pp. 4140–4155, 2018.

[15] Z. Han, L. Wang, and Z. Lin, "Local formation control strategies with undetermined and determined formation scales for co-leader vehicle networks," in *52nd IEEE Conference on Decision and Control*. IEEE, 2013, pp. 7339–7344.

[16] L. Quan, L. Yin, C. Xu, and F. Gao, "Distributed swarm trajectory optimization for formation flight in dense environments," in *2022 International Conference on Robotics and Automation (ICRA)*. IEEE, 2022, pp. 4979–4985.

[17] A. T. Nguyen, J.-W. Lee, T. B. Nguyen, and S. K. Hong, "Collision-free formation control of multiple nano-quadrotors," *arXiv preprint arXiv:2107.13203*, 2021.

[18] Y. Zhou, L. Quan, C. Xu, G. Xu, and F. Gao, "Sparse-graph-enabled formation planning for large-scale aerial swarms," *arXiv preprint arXiv:2403.17288*, 2024.

[19] J. Alonso-Mora, E. Montijano, M. Schwager, and D. Rus, "Distributed multi-robot formation control among obstacles: A geometric and optimization approach with consensus," in *2016 IEEE international conference on robotics and automation (ICRA)*. IEEE, 2016, pp. 5356–5363.

[20] J. Tordesillas and J. P. How, "Panther: Perception-aware trajectory planner in dynamic environments," *IEEE Access*, vol. 10, pp. 22 662–22 677, 2022.

[21] ———, "Deep-panther: Learning-based perception-aware trajectory planner in dynamic environments," *IEEE Robotics and Automation Letters*, vol. 8, no. 3, pp. 1399–1406, 2023.

[22] X. Zhou, J. Zhu, H. Zhou, C. Xu, and F. Gao, "Ego-swarm: A fully autonomous and decentralized quadrotor swarm system in cluttered environments," in *2021 IEEE international conference on robotics and automation (ICRA)*. IEEE, 2021, pp. 4101–4107.

[23] X. Zhou, X. Wen, Z. Wang, Y. Gao, H. Li, Q. Wang, T. Yang, H. Lu, Y. Cao, C. Xu, et al., "Swarm of micro flying robots in the wild," *Science Robotics*, vol. 7, no. 66, p. eabm5954, 2022.

[24] C. Tounieh and D. Floreano, "High-speed motion planning for aerial swarms in unknown and cluttered environments," *arXiv preprint arXiv:2402.19033*, 2024.

[25] G. Vásárhelyi, C. Virág, G. Somorjai, T. Nepusz, A. E. Eiben, and T. Vicsek, "Optimized flocking of autonomous drones in confined environments," *Science Robotics*, vol. 3, no. 20, p. eaat3536, 2018.

[26] R. J. Amala Arokia Nathan, I. Kurmi, and O. Bimber, "Drone swarm strategy for the detection and tracking of occluded targets in complex environments," *Communications Engineering*, vol. 2, no. 1, p. 55, 2023.

[27] D. Wang, T. Fan, T. Han, and J. Pan, "A two-stage reinforcement learning approach for multi-uav collision avoidance under imperfect sensing," *IEEE Robotics and Automation Letters*, vol. 5, no. 2, pp. 3098–3105, 2020.

[28] J. Alonso-Mora, T. Naegeli, R. Siegwart, and P. Beardsley, "Collision avoidance for aerial vehicles in multi-agent scenarios," *Autonomous Robots*, vol. 39, pp. 101–121, 2015.

[29] J. Tordesillas and J. P. How, "Mader: Trajectory planner in multiagent and dynamic environments," *IEEE Transactions on Robotics*, vol. 38, no. 1, pp. 463–476, 2021.

[30] K. Kondo, R. Figueiroa, J. Rached, J. Tordesillas, P. C. Lusk, and J. P. How, "Robust mader: Decentralized multiagent trajectory planner robust to communication delay in dynamic environments," *IEEE Robotics and Automation Letters*, 2023.

[31] K. Kondo, C. T. Tewari, M. B. Peterson, A. Thomas, J. Kinnari, A. Tagliabue, and J. P. How, "Puma: Fully decentralized uncertainty-aware multiagent trajectory planner with real-time image segmentation-based frame alignment," *arXiv preprint arXiv:2311.03655*, 2023.

[32] B. B. Şenbaşlar, "Decentralized real-time trajectory planning for multi-robot navigation in cluttered environments," Ph.D. dissertation, University of Southern California, 2023.

[33] B. Şenbaşlar, P. Luiz, W. Hönig, and G. S. Sukhatme, "Mrnav: Multi-robot aware planning and control stack for collision and deadlock-free navigation in cluttered environments," *arXiv preprint arXiv:2308.13499*, 2023.

[34] Z. Huang, Z. Yang, R. Krupani, B. Şenbaşlar, S. Batra, and G. S. Sukhatme, "Collision avoidance and navigation for a quadrotor swarm using end-to-end deep reinforcement learning," *arXiv preprint arXiv:2309.13285*, 2023.

[35] E. Kaufmann, L. Bauersfeld, and D. Scaramuzza, "A benchmark comparison of learned control policies for agile quadrotor flight," in *2022 International Conference on Robotics and Automation (ICRA)*. IEEE, 2022, pp. 10 504–10 510.

[36] C. Yu, A. Vélu, E. Vinitsky, Y. Wang, A. Bayen, and Y. Wu, "The surprising effectiveness of ppo in cooperative, multi-agent games. arxiv 2021," *arXiv preprint arXiv:2103.01955*.

[37] L. Quan, L. Yin, T. Zhang, M. Wang, R. Wang, S. Zhong, X. Zhou, Y. Cao, C. Xu, and F. Gao, "Robust and efficient trajectory planning for formation flight in dense environments," *IEEE Transactions on Robotics*, 2023.

[38] B. Xu, F. Gao, C. Yu, R. Zhang, Y. Wu, and Y. Wang, "Omnidrones: An efficient and flexible platform for reinforcement learning in drone control," *IEEE Robotics and Automation Letters*, 2024.